Lab on a Chip

View Online
Dynamic Article Links

Cite this: *Lab Chip*, 2011, **11**, 2066

www.rsc.org/loc

PAPER

On-chip background noise reduction for cell-based assays in droplets†

Pascaline Mary,[a] Angela Chen,[a] Irwin Chen,[b] Adam R. Abate[a] and David A. Weitz*[a]

Received 24th February 2011, Accepted 4th April 2011
DOI: 10.1039/c1lc20159j

Droplet-based microfluidics provides an excellent platform for high-throughput biological assays. Each droplet serves as a reaction vessel with a volume as small as a few picolitres. This is an important technology for a high variety of applications. However this technology is restricted to homogeneous assays as it is very difficult to wash reagents from the reaction vessel. To help overcome this limitation, we introduce a method to effectively dilute the content of a droplet while retaining the high throughput. We use electrocoalescence to merge the parent drop with a much larger drop containing only solvent, thereby increasing the volume of the drop by as much as a factor of 14. Three T-junctions then break the larger drop into eight smaller droplets. This dilution and break-up process can be repeated, thus leading to many drops comparable in size to the original one but with much lower concentration of reagents. The system is fully integrated in a PDMS device. To demonstrate its power, we perform a labelling reaction at the surface of the cells by coencapsulating yeast cells expressing S6 peptide tags with the enzyme SFP synthase and the fluorescent substrate CoA 488. After reaction, the droplets are diluted twice using the system and the intensity of their fluorescence is measured. This noise reduction method enables us to more easily distinguish the fluorescence at the surface of a single cell from the fluorescent background inside the droplet.

Introduction

The use of droplet-based microfluidics to miniaturize chemical and biological screening is an important area of research.[1–3] Each drop can serve as a picolitre test-tube within which individual reactions can be performed.[4] This technology offers interesting features for cell-based assays: the reduction of volume is well adapted to the single-cell level and reduces the reagents consumption with a high degree of control. Droplet-based microfluidics has already shown great promise for cell-based assays: cells can be encapsulated with reagents,[5] incubated[6] and sorted;[7,8] reagents can be added at different times[9,10] and the assay can be probed on chip.[11] However, the inability to perform washing steps to remove excess reagents limits to homogeneous assays and remains a major obstacle for performing multi-step reactions or integrating an online reaction and detection step. Up until now, most of the washing steps developed in microfluidics use magnetic beads to isolate reagents of interest.[12–14] This method is applicable to cells: by conjugating peptide, antibody or lectin coated magnetic particles at a surface of a cell[15,16] or by phagocytosis of the beads.[17] Magnetic actuators can be miniaturized due to the possible high magnetic field gradient in microchannels.[18] A drawback to using magnetic particles in microfluidic systems is that appropriate micro-manipulating systems need to be implemented to control the magnetic field.

In this work, we present a method working at high-throughput that is able to dilute up to 14 times droplets. The system uses dielectrophoresis to quantitatively inject reagents into droplets. The larger droplet is then split into eight smaller droplets by three consecutive T-junctions. We apply this method to detect a site specific protein labeling reaction mediated by an enzyme and occurring at the surface of a yeast. By repeating the dilution-break up process twice, we are able to reduce the level of background noise 100 times within a droplet. This platform avoids any off-chip handling procedure, often the source of reagent loss, longer response time and cross-contamination.

Materials and methods

Fabrication of the microfluidic devices

The microfluidic devices are fabricated with poly(dimethylsiloxane) (PDMS) using soft-lithography techniques.[19] The droplet-dilution module requires electrodes to trigger dilution. To make the electrodes, we fabricate microchannels with the desired shape; we heat the device and inject a low melting-point liquid solder into these channels.[20] Upon cooling to room temperature, the solder becomes solid, producing the electrodes. We make electrical connections using eight-pin terminal blocks (Digikey) glued to the surface of the device for strain relief

[a]*School of Engineering and Applied Sciences/Department of Physics, Harvard University, Cambridge, Massachusetts, USA. E-mail: weitz@seas.harvard.edu; Tel: +1-617-495-3275*
[b]*Department of Chemistry and Chemical Biology, Harvard University, Cambridge, Massachusetts, USA*

† Electronic supplementary information (ESI) available: Movies of the drop dilution and splitting steps. See DOI: 10.1039/c1lc20159j

(Loctite UV cured). The voltage is applied with a function generator producing pulses at 20 kHz and amplified by a factor of 1000 by a high-voltage amplifier (Trek).

Microfluidic device operation

Three separate devices are used. A schematic of the different chips used is represented in Fig. 1. The flows of the fluids are controlled by syringe pumps (PHD 22/2000, Harvard Apparatus). The module forming droplets uses a flow-focusing junction with a 25 × 25 μm nozzle; it is shown in Fig. 1a–c. Droplets are produced in a fluorinated oil (HFE 7500, 3M, St Paul, Minnesota) containing 1.8% (wt/wt) of EA surfactant[21] (Raindance Technologies). We collect the emulsion in a 500 μL glass syringe (Hamilton gastight). The dilution and the subsequent break-up is performed in a separate device (see Fig. 1d–f), where droplets are spaced by a flow of oil and enter a 50 μm wide by 40 μm high channel that forces them to flow into a single line. Near the electrodes, a T-junction connects the droplet channel to a second injection channel; the droplets are merged with a much larger droplet formed at the second junction. After dilution, three successive T-junctions break the drops symmetrically into smaller drops. These smaller drops can be reinjected into a third module, which is the detection module, represented in Fig. 1g and h; here they are spaced out by an additional flow of oil and the intensity of their fluorescence is detected.

Droplet detection and analysis

The detection module is placed on an inverted microscope and the fluorescence is detected with a photomultiplicator (PMT) attached to its epifluorescent port. The fluorescence is excited by a laser beam (Picarro, 20 mW cyan laser) aligned with the optical axis of the microscope and focused on the sample by a 40× objective. The drops pass through a 15 μm wide and 20 μm high channel where they are detected. The data are collected with a DAQ card (NI Corporation) controlled through Labview (NI corporation). In addition, fluorescent images of static drops are obtained with an EM-CCD camera (Qimaging Rolera MGI).

Reagents in droplets

The dilution is measured using a solution of fluorescein at 1 mM buffered at pH 7.4 with 1× tris buffered saline (TBS). The drops are diluted with pure 1× TBS. The enzymatic assay in the drops is performed using a droplet maker with two inlet channels, one containing the yeast suspension and the other containing the substrate and enzyme. Yeasts are grown in YPD medium (Yeast Extract Peptone Dextrose). The cell density is measured and the cells are centrifuged twice and resuspended at the appropriate concentration in TBS containing 1 mg mL^{-1} of bovine serum albumin (BSA). The suspension is completed with 35% (v/v) Optiprep (Axis-Shield), a density gradient medium, to match the density of the yeast with the surrounding liquid and prevent sedimentation. The reagent solution is composed of 40 mM of 4′-phosphopantetheinyl transferase (SFP synthase), 10 mM of CoA-488 (New Englands Biolabs), 10 mM of $MgCl_2$ and 780 μg. mL^{-1} of BSA.

Results

Droplets containing fluorescein are produced at high-volume fraction in the drop-maker module and reinjected into the dilution/splitting module using a piece of tubing that connects the devices. The synchronization between the reagent drop reinjection and the injection of the dilution buffer is achieved by adjusting the flow rate of the oil between the drops. When a reagent drop flows by the injector channel and reaches the

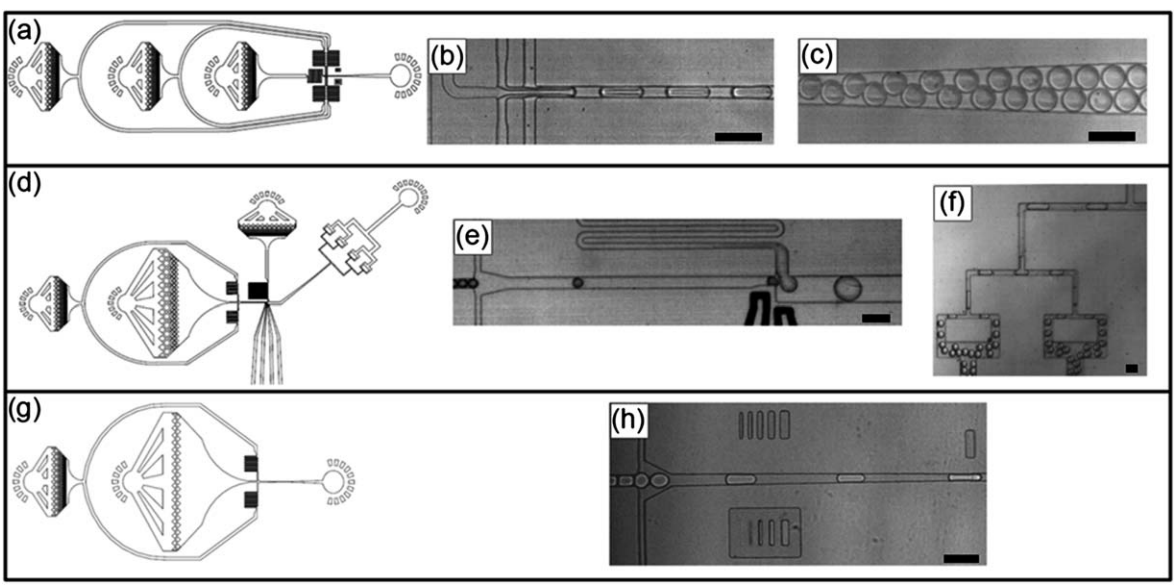

Fig. 1 Microfluidic devices and functions. (a) Schematic representation of the drop maker. (b) Bright field image of the flow focusing junction. (c) Bright field image of 40 μm droplets flowing in the channel. (d) Schematic representation of the dilution/splitting device. (e) Bright field image of the dilution area. (f) Bright field image of droplet breakup at the T junctions. (g) Schematic representation of the detection device. (h) Bright field image of the detection channel. Scale bars: 100 μm.

incoming buffer stream, an electric field is generated to destabilize their interface causing the drop to merge with the injected fluid. As the incoming dilution buffer stream continues to grow, it ultimately detaches from the stream to form a large drop, as shown in Fig. 1e and the movie in the ESI†. The flow rate of the continuous phase oil affects both the spacing between the incoming reagent drops and the size and frequency of the large drops formed from the dilution buffer. For a constant flow rate of reagent drops, increasing the flow rate of the continuous phase leads to a decrease in the formation of the large buffer drops; it also increases the spacing between consecutive reagent drops while simultaneously increasing their speed. Thus, to maintain a given dilution ratio, the flow rate of the continuous phase oil must be optimized to obtain one-to-one droplet fusion.

We use image analysis to determine the radii of the drops, thereby measuring the dilution ratio. This ratio is equal to $(Q_{inject} + Q_{drop})/Q_{drop}$, where Q_{drop} and Q_{inject} are the flow rate of the reagent drops and of the injected buffer respectively, as shown in Fig. 2a. The maximum dilution achieved is 14×. Above this value, synchronization of the two drop streams becomes difficult; moreover the high flow rate of the continuous phase oil generates an excessive pressure in the channels, which deforms them.

To evaluate sources of variability in the dilution, we measure the standard deviation in the volume injected and plot this as error bars in Fig. 2a. The standard deviation is ~5% of the total volume and is attributed to fluctuations of the injected volume.

To control the dilution ratio we adjust the ratio between Q_{inject} and Q_{drop}. The ratio between the concentration of fluorescein in the droplets before (C_{inital}) and after (C_{final}) dilution is determined by

$$\frac{C_{final}}{C_{initial}} = \frac{Q_{drop}}{Q_{drop} + Q_{inject}} \quad (1)$$

After dilution, the large drops are broken into smaller drops in three consecutive T-junctions, each of which provides a reduction in droplet volume by a factor of two; this leads to a final drop that is one eighth of the original. At high injection rate of the reagents, satellite drops are produced by secondary breakup events at the T-junction; this limits the droplet injection flow rate to 100 $\mu L.h^{-1}$.

The intensity of fluorescence emitted by the drop is recorded after collection and reinjection into the detection device. The distributions of fluorescence intensity of drops initially containing 1 μM fluorescein and from drops diluted by factors of 6, 8 and 10 times are shown Fig. 2b. The distributions each exhibit a distinct maximum, which corresponds to the specific fluorescein concentration in that set of drops. We estimate the number of unfused droplets to be ~3%. Drops fused two-to-one (two assay drops fused to one dilution drop), contribute to the standard deviation of the peaks. The standard deviation of the diluted is ~5 times larger than that of drops containing the same fluorescein concentration but formed and detected without dilution.

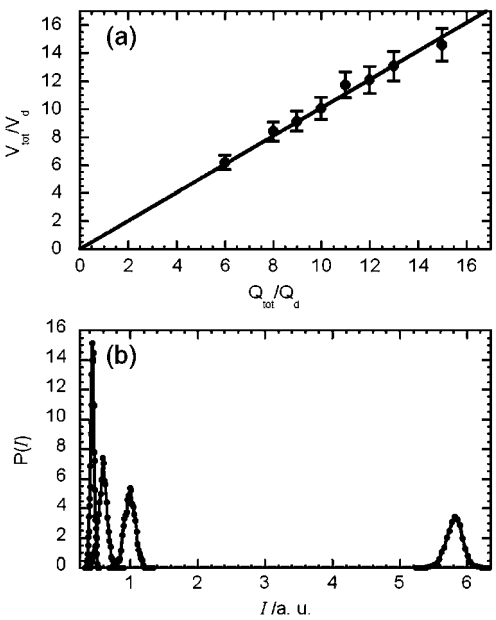

Fig. 2 (a) Ratio of the volumes between after and before injection as a function of the sum of the droplet and injection flow rate divided by the droplet flow rate. (b) Normalized distribution of the fluorescence intensity of the drops initially at 1 μM in fluorescein, after 6, 8 and 10 times dilution and without dilution.

Enzymatic assay: SFP labeling reaction

Fluorometric assays are widely used to quantify enzymatic reactions. Fluorescence resonance energy transfer (FRET) is a way to avoid washing steps before measurements. However, FRET has a limited dynamic range compared to detection of fluorescence. Furthermore, FRET requires pre-labeling the surface with a fluorophore, which may not always be possible in a reproducible manner. Because of these limitations, measurement of fluorescence can be preferable. To demonstrate the potentiality of the dilution platform, we present a fluorescent labeling reaction at the surface of cells.

Expression of the S6 peptide sequence on the cell surface enables fluorescent labeling of yeast using SFP synthase.[22] In the labeling reaction, the Alexa Fluor488-substituted phosphopantetheine group of the CoA-488 substrate is covalently transferred to the serine side chain within the S6 sequence by the enzyme SFP synthase (Fig. 3). In the absence of washing, distinguishing the intensity of bulk and surface fluorescence requires

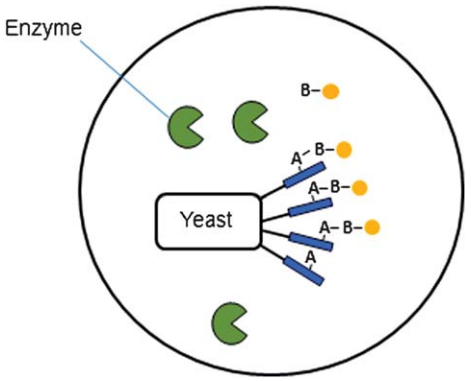

Fig. 3 Schematic representation of the enzymatic assay in droplets. A represents the S6 peptide tag and B represents the CoA substrate.

precise adjustment of the concentration of fluorescent substrate to ensure that the number of ligated molecules is larger than those unreacted. This restricts the operation to a non-ideal range of concentrations. The dilution strategy introduced here significantly reduces only the concentration of the unreacted fluorophores. This increases the relative signal of the fluorescence of the cell compared to the background of those drops containing cells. Despite the fact that only one drop out of eight contains a cell, the reduction of the overall background noise is a significant improvement.

To perform the enzymatic assay in drops, we coflow a suspension of yeast cells engineered to display the S6 peptide[23] with a second stream containing SFP synthase and the CoA-488 substrate. The enzymatic reaction begins after formation of the drop, when the two streams mix. Before dilution, the average cell concentration is 3 cells per drop and the drop diameter is 45 μm. The drops are incubated overnight and reinjected into the dilution/splitting module. Drops are diluted twice, resulting in a 100 times reduction in the concentration of unreacted fluorophores. Bright field images of drops containing a cell before dilution, diluted 10 times and diluted 100 times are shown in Fig. 4a–c, respectively; the corresponding fluorescence images are shown in Fig. 4d–f. A 100 times dilution ensures a sufficient reduction in noise to enable the easy detection of the cell. As shown in the inset of Fig. 4g, the detection of a cell within a drop results in a voltage peak; this peak is shorter and more intense than that due to the drop itself. The fluorescence-intensity distribution is a bimodal distribution (Fig. 4g); the mode centered on $I = 0.142$ corresponds to the detection of the bulk fluorescence, whereas the mode centered on $I = 0.256$ corresponds to the detection of fluorescence at the surface of the cells. The total number of counts corresponding to the detection of cells is 15% smaller than the value predicted; this difference is attributed to the uncertainty in the cell density measurement and to the presence of cells aggregates that are counted as a single cell.

The large number of empty drops that result from breakup could be eliminated using a detection and sorting module if desired.

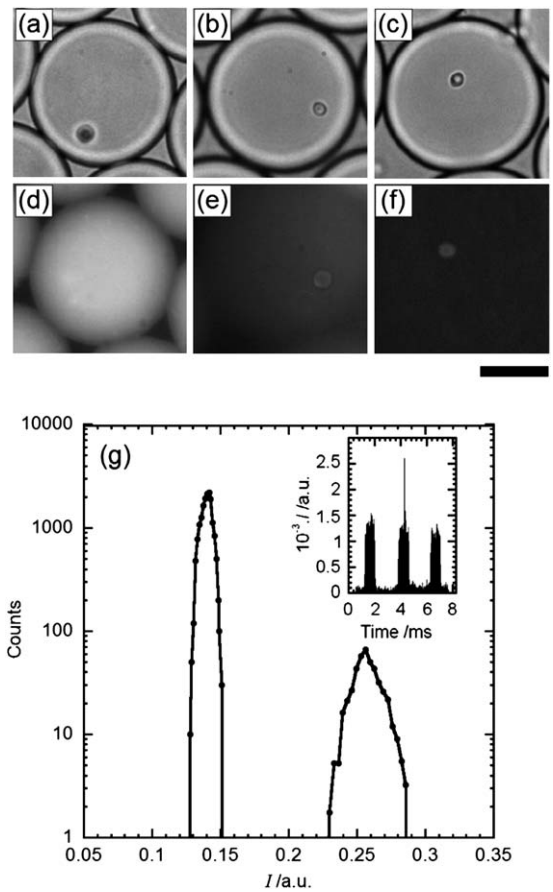

Fig. 4 Enzymatic assay in droplets. (a), (b) and (c) correspond to a bright field image of a droplet containing one cell before dilution, after 10 times and after 100 times dilution respectively. (d), (e) and (f) are the corresponding fluorescent images. Scale bar: 20 μm. (g) Histogram of the intensity of fluorescence after 100 times dilution. The first peak centered on $I = 0.142$ corresponds to the fluorescent background within the drops. The brightest peak, centered on $I = 0.256$ corresponds to the fluorescence intensity of the cells.

Conclusions

The microfluidic platform presented in this work provides a means to significantly decrease the background noise when performing cell-based assays in drops. The washing step is performed by controllably diluting the content of the drops using electrocoalescence; it is followed by drop breakup to reduce the size of the diluted drop. This device is able to screen cells at high-throughput without any external washing step, which would require breaking the emulsion, a potential source of significant loss of cells.

This device has the potential of providing significantly improved signal to noise in high-throughput screening applications in drop-based microfluidics.

Acknowledgements

This work was supported by the NSF (DMR-1006546), the Harvard MRSEC (DMR-0820484), and the Massachusetts Life Sciences Center. The authors also thank Saint-Gobain Recherche for financial support.

Notes and references

1 S. Vyawahare, A. D. Griffiths and C. A. Merten, *Chem. Biol.*, 2010, **17**, 1052–1065.
2 H. Song, D. L. Chen and R. F. Ismagilov, *Angew. Chem., Int. Ed.*, 2006, **45**, 7336–7356.
3 D. T. Chiu and R. M. Lorenz, *Acc. Chem. Res.*, 2009, **42**, 649–658.
4 R. Tewhey, J. B. Warner, M. Nakano, B. Libby, M. Medkova, P. H. David, S. K. Kotsopoulos, M. L. Samuels, J. B. Hutchison, J. W. Larson, E. J. Topol, M. P. Weiner, O. Harismendy, J. Olson, D. R. Link and K. A. Frazer, *Nat. Biotechnol.*, 2009, **27**, 1025–U1094.
5 J. C. Baret, Y. Beck, I. Billas-Massobrio, D. Moras and A. D. Griffiths, *Chem. Biol.*, 2010, **17**, 528–536.
6 S. Koster, F. E. Angile, H. Duan, J. J. Agresti, A. Wintner, C. Schmitz, A. C. Rowat, C. A. Merten, D. Pisignano, A. D. Griffiths and D. A. Weitz, *Lab Chip*, 2008, **8**, 1110–1115.
7 J. J. Agresti, E. Antipov, A. R. Abate, K. Ahn, A. C. Rowat, J. C. Baret, M. Marquez, A. M. Klibanov, A. D. Griffiths and D. A. Weitz, *Proc. Natl. Acad. Sci. U. S. A.*, 2010, **107**, 4004–4009.
8 J. C. Baret, O. J. Miller, V. Taly, M. Ryckelynck, A. El-Harrak, L. Frenz, C. Rick, M. L. Samuels, J. B. Hutchison, J. J. Agresti, D. R. Link, D. A. Weitz and A. D. Griffiths, *Lab Chip*, 2009, **9**, 1850–1858.

9 L. Mazutis, J. C. Baret, P. Treacy, Y. Skhiri, A. F. Araghi, M. Ryckelynck, V. Taly and A. D. Griffiths, *Lab Chip*, 2009, **9**, 2902–2908.
10 A. R. Abate, T. Hung, P. Mary, J. J. Agresti and D. A. Weitz, *Proc. Natl. Acad. Sci. U. S. A.*, 2010, **107**, 19163–19166.
11 E. Brouzes, M. Medkova, N. Savenelli, D. Marran, M. Twardowski, J. B. Hutchison, J. M. Rothberg, D. R. Link, N. Perrimon and M. L. Samuels, *Proc. Natl. Acad. Sci. U. S. A.*, 2009, **106**, 14195–14200.
12 J. S. Marcus, W. F. Anderson and S. R. Quake, *Anal. Chem.*, 2006, **78**, 3084–3089.
13 A. Russom, N. Tooke, H. Andersson and G. Stemme, *Anal. Chem.*, 2005, **77**, 7505–7511.
14 R. S. Sista, A. E. Eckhardt, V. Srinivasan, M. G. Pollack, S. Palanki and V. K. Pamula, *Lab Chip*, 2008, **8**, 2188–2196.
15 M. Imbeault, R. Lodge, M. Ouellet and M. J. Tremblay, *Virology*, 2009, **393**, 160–167.
16 I. Safarik and M. Safarikova, *J. Chromatogr., Biomed. Appl.*, 1999, **722**, 33–53.
17 O. Burkhardt and H. J. Merker, *Ann. Anat.*, 2002, **184**, 55–60.
18 B. Teste, F. Malloggi, A.-L. Gassner, T. Georgelin, J.-M. Siaugue, A. Varenne, H. Girault and S. Descroix, *Lab Chip*, 2011, **11**, 833–840.
19 D. C. Duffy, J. C. McDonald, O. J. A. Schueller and G. M. Whitesides, *Anal. Chem.*, 1998, **70**, 4974–4984.
20 A. C. Siegel, D. A. Bruzewicz, D. B. Weibel and G. M. Whitesides, *Adv. Mater.*, 2007, **19**, 727.
21 C. Holtze, A. C. Rowat, J. J. Agresti, J. B. Hutchison, F. E. Angile, C. H. J. Schmitz, S. Koster, H. Duan, K. J. Humphry, R. A. Scanga, J. S. Johnson, D. Pisignano and D. A. Weitz, *Lab Chip*, 2008, **8**, 1632–1639.
22 Z. Zhou, P. Cironi, A. J. Lin, Y. Q. Xu, S. Hrvatin, D. E. Golan, P. A. Silver, C. T. Walsh and J. Yin, *ACS Chem. Biol.*, 2007, **2**, 337–346.
23 I. Chen, B. M. Dorr and D. R. Liu, 2011, submitted.

